JVI Journals.ASM.org

Attenuating Mutations in nsP1 Reveal Tissue-Specific Mechanisms for Control of Ross River Virus Infection

Kristina A. Stoermer Burrack,[b,d] David W. Hawman,[a,c] Henri J. Jupille,[a,c] Lauren Oko,[a] Marissa Minor,[a]* Katherine D. Shives,[a,d] Bronwyn M. Gunn,[e] Kristin M. Long,[f] Thomas E. Morrison[a,b]

Department of Microbiology, University of Colorado School of Medicine, Aurora, Colorado, USA[a]; Department of Immunology, University of Colorado School of Medicine, Aurora, Colorado, USA[b]; Graduate Program in Microbiology, University of Colorado School of Medicine, Aurora, Colorado, USA[c]; Graduate Program in Immunology, University of Colorado School of Medicine, Aurora, Colorado, USA[d]; Department of Microbiology and Immunology, University of North Carolina at Chapel Hill, Chapel Hill, North Carolina, USA[e]; Department of Genetics, University of North Carolina at Chapel Hill, Chapel Hill, North Carolina, USA[f]

ABSTRACT

Ross River virus (RRV) is one of a group of mosquito-transmitted alphaviruses that cause debilitating, and often chronic, musculoskeletal disease in humans. Previously, we reported that replacement of the nonstructural protein 1 (nsP1) gene of the mouse-virulent RRV strain T48 with that from the mouse-avirulent strain DC5692 generated a virus that was attenuated in a mouse model of disease. Here we find that the six nsP1 nonsynonymous nucleotide differences between strains T48 and DC5692 are determinants of RRV virulence, and we identify two nonsynonymous nucleotide changes as sufficient for the attenuated phenotype. RRV T48 carrying the six nonsynonymous DC5692 nucleotide differences (RRV-T48-nsP1^{6M}) was attenuated in both wild-type and *Rag1*$^{-/-}$ mice. Despite the attenuated phenotype, RRV T48 and RRV-T48-nsP1^{6M} loads in tissues of wild-type and *Rag1*$^{-/-}$ mice were indistinguishable from 1 to 3 days postinoculation. RRV-T48-nsP1^{6M} loads in skeletal muscle tissue, but not in other tissues, decreased dramatically by 5 days postinoculation in both wild-type and *Rag1*$^{-/-}$ mice, suggesting that the RRV-T48-nsP1^{6M} mutant is more sensitive to innate antiviral effectors than RRV T48 in a tissue-specific manner. *In vitro*, we found that the attenuating mutations in nsP1 conferred enhanced sensitivity to type I interferon. In agreement with these findings, RRV T48 and RRV-T48-nsP1^{6M} loads were similar in mice deficient in the type I interferon receptor. Our findings suggest that the type I IFN response controls RRV infection in a tissue-specific manner and that specific amino acid changes in nsP1 are determinants of RRV virulence by regulating the sensitivity of RRV to interferon.

IMPORTANCE

Arthritogenic alphaviruses, including Ross River virus (RRV), infect humans and cause debilitating pain and inflammation of the musculoskeletal system. In this study, we identified coding changes in the RRV nsP1 gene that control the virulence of RRV and its sensitivity to the antiviral type I interferon response, a major component of antiviral defense in mammals. Furthermore, our studies revealed that the effects of these attenuating mutations are tissue specific. These findings suggest that these mutations in nsP1 influence the sensitivity of RRV to type I interferon only in specific host tissues. The new knowledge gained from these studies contributes to our understanding of host responses that control alphavirus infection and viral determinants that counteract these responses.

Ross River virus (RRV) is a positive-sense, single-stranded RNA virus in the *Alphavirus* genus of the family *Togaviridae* (1). RRV is one of a group of related mosquito-transmitted alphaviruses, including chikungunya virus (CHIKV), Mayaro virus, o'nyong-nyong virus, and others, that typically cause a debilitating musculoskeletal inflammatory disease in humans. These viruses are emerging disease threats due to their ability to cause explosive epidemics. Past epidemics include a 1979-to-1980 epidemic of RRV disease in the South Pacific that involved more than 60,000 patients (2) and a 1959-to-1962 epidemic of o'nyong-nyong fever in Africa that involved at least 2 million infections (3). Since 2004, CHIKV has caused major epidemics in multiple countries in the Indian Ocean region, with estimates on the order of 1 million to 6 million cases (4).

Clinical manifestations following infection with arthritis/myositis-associated alphaviruses develop following an incubation period ranging from 2 to 12 days (2, 5). The disease is most commonly characterized by fever, intense pain in the peripheral joints, myalgias, and an impaired ability to ambulate (2, 6, 7). A number of studies indicate that musculoskeletal pain lasts for months to years in a subset of persons infected with RRV or CHIKV; however, the cause of these long-lasting symptoms is unclear (2, 8–12). There are currently no licensed antivirals or vaccines for any of the arthritis/myositis-associated alphaviruses. Treatment is limited to supportive care with analgesics and anti-inflammatory drugs (2, 5).

To study the pathogenesis of arthritis/myositis-associated alphaviruses, we have developed mouse models of RRV- and

Received 10 December 2013 **Accepted** 7 January 2014
Published ahead of print 15 January 2014
Editor: B. Williams
Address correspondence to Thomas E. Morrison, thomas.morrison@ucdenver.edu.
* Present address: Marissa Minor, Department of Molecular Virology and Microbiology, Baylor College of Medicine, Houston, Texas, USA.
Supplemental material for this article may be found at http://dx.doi.org/10.1128/JVI.02609-13.

doi:10.1128/JVI.02609-13

CHIKV-induced disease that recapitulate many aspects of the human diseases (13–17). Studies with the RRV mouse model demonstrated that following a high-titer serum viremia, bone/joint-associated tissues and skeletal muscle tissue are the primary targets of RRV replication (15, 18). RRV replication at these sites results in a severe inflammatory response with abundant tissue damage, leading to deficits in grip strength and an altered gait. Human disease following infection by an arthritogenic alphavirus shows a similar progression, with (i) high-titer serum viremia (19, 20), (ii) the detection of virus RNA and/or antigen in musculoskeletal tissues (21, 22), (iii) mononuclear inflammatory infiltrates in joints and muscle tissue (19, 22–24), and (iv) disease signs, such as musculoskeletal pain and difficulty ambulating. Thus, understanding the host and viral factors that contribute to pathogenesis in this mouse model may aid in the development of therapies and vaccines to treat or prevent human disease.

Previously, we reported that replacement of the nonstructural protein 1 (nsP1) coding region of RRV T48 with that from the mouse-avirulent strain DC5692 resulted in an attenuated phenotype in the mouse model (25). Here we find that the six nsP1 nonsynonymous nucleotide differences between strains T48 and DC5692 are determinants of RRV virulence, and we identify two nonsynonymous nucleotide changes as sufficient for the attenuated phenotype. RRV T48 encoding the six nonsynonymous DC5692 nucleotides (RRV-T48-nsP1^{6M}) was attenuated in wild-type (WT) and *Rag1*$^{-/-}$ mice. RRV-T48-nsP1^{6M} loads in the tissues of WT and *Rag1*$^{-/-}$ mice were similar to those of the virulent virus RRV T48 from 1 to 3 days postinoculation (dpi) but declined sharply in skeletal muscle tissue, but not in joint tissue, by 5 dpi, suggesting that the RRV-T48-nsP1^{6M} mutant is more sensitive to innate antiviral effectors in a tissue-specific manner. *In vitro*, we found that the attenuating mutations in nsP1 conferred enhanced sensitivity to type I interferon (IFN). In agreement with these findings, RRV T48 and RRV-T48-nsP1^{6M} loads in skeletal muscle tissue and their virulence were similar in mice deficient in the type I IFN receptor. Our findings suggest that specific amino acid changes in nsP1 are determinants of RRV virulence by regulating the sensitivity of RRV to IFN and that type I IFN controls RRV infection in a tissue-specific manner.

MATERIALS AND METHODS

Viruses. The T48 strain of RRV (GenBank accession no. GQ433359) was isolated from *Aedes vigilax* mosquitoes in Queensland, Australia. Prior to cDNA cloning, the virus was passaged 10 times in suckling mice, followed by 2 passages in Vero cells (26, 27). Thus, this strain may be adapted for enhanced virulence in mice. RRV strain DC5692 (GenBank accession no. HM234643) was isolated in 1995 from *Aedes camptorhynchus* mosquitoes at Dawesville Cut in the Peel region of Western Australia (28). The virus was passaged once in C6/36 cells, once in Vero cells, and once in BHK-21 cells prior to cDNA cloning (25).

Virus stocks were generated from cDNAs as described previously (15). Briefly, plasmids encoding virus cDNAs were linearized by digestion with SacI. 5′-capped full-length RNA transcripts were generated *in vitro* using SP6-specific mMessage mMachine *in vitro* transcription kits (Ambion). Full-length transcripts were electroporated into BHK-21 cells using a Bio-Rad Gene Pulser electroporator. Culture supernatants were harvested at 24 h after electroporation, centrifuged for 20 min at 3,000 rpm (relative centrifugal force [RCF], 1,721 × *g*), aliquoted, and stored at −80°C. Viral stocks were titrated by plaque assays on BHK-21 cells.

Construction of virus cDNAs. Plasmid pRR64 (provided by Richard Kuhn, Purdue University) encodes the full-length cDNA of the T48 strain of RRV (27). The generation of pRR94 (encoding RRV-T48-nsP1^{DC5692}) and pRR108 (encoding RRV-DC5692-PE2^{T48}) has been described previously (25). To generate virus cDNAs with specific mutations in nsP1, a shuttle vector (pRR90) was created by religation of pRR64 that had been digested with EcoRI. The six nonsynonymous mutations in the strain DC5692 nsP1 coding region were introduced sequentially into pRR90 via site-directed mutagenesis using the QuikChange II XL site-directed mutagenesis kit (Agilent Technologies). Following sequence analysis, pRR90 BssHII-EagI fragments carrying various mutations in nsP1 were inserted into the BssHII-EagI sites of pRR64. A similar strategy, involving the sequential introduction of the nonsynonymous T48 strain nsP1 nucleotide changes into a shuttle vector derived from pRR108, followed by subcloning of the BssHII-XbaI fragment, was utilized to generate pRR112, encoding RRV-DC5692-nsP1^{6M}-PE2^{T48}.

Cells. BHK-21 cells (ATCC CCL10) were grown in α-minimal essential medium (Gibco) supplemented with 10% bovine calf serum (HyClone), 10% tryptose phosphate broth, penicillin and streptomycin, and 0.29 mg/ml L-glutamine. Vero cells (ATCC CCL81) were grown in Dulbecco's modified Eagle medium (DMEM)–F-12 medium (Gibco) supplemented with 10% fetal bovine serum (FBS) (Lonza), nonessential amino acids (Gibco), sodium bicarbonate, penicillin and streptomycin, and 0.29 mg/ml L-glutamine. C2C12 murine muscle cells were cultured in DMEM supplemented with 10% FBS. C2C12 cells were differentiated into myotubes by culturing in fusion medium (DMEM–2% horse serum) for 5 to 6 days. L929 cells were grown in DMEM supplemented with 10% FBS, penicillin and streptomycin, and 0.29 mg/ml L-glutamine.

Plaque assays. BHK-21 cells or Vero cells were seeded into 6-well dishes. The growth medium was removed, and cell monolayers were inoculated with serial 10-fold dilutions of virus-containing samples. Following a 1-h adsorption at 37°C, cell monolayers were overlaid with 0.5% immunodiffusion agarose (MP Biomedicals) in medium for 38 to 40 h, and plaques were visualized by staining with neutral red (Sigma).

Mouse experiments. WT, *Rag1*$^{-/-}$, and *Ifng*$^{-/-}$ C57BL/6J mice were obtained from The Jackson Laboratory (Bar Harbor, ME) and were bred in-house. C57BL/6 *Ifnar1*$^{-/-}$ mice were provided by Ken Tyler and Mario Santiago, University of Colorado School of Medicine. Animal husbandry and experiments were performed in accordance with all University of Colorado School of Medicine and University of North Carolina Institutional Animal Care and Use Committee guidelines. Although RRV is classified as a biosafety level 2 pathogen, due to its exotic nature all mouse studies were performed in an animal biosafety level 3 laboratory. Unless otherwise indicated, 3- to 4-week-old mice were used for all *in vivo* studies. Mice were inoculated in the left rear footpad with 10^3 PFU of virus in a diluent (phosphate-buffered saline [PBS]–1% bovine calf serum) in a 10-μl volume. Mock-infected animals received the diluent alone. Mice were monitored for disease signs and were weighed at 24-h intervals. Disease scores were determined by assessing grip strength, hind limb weakness, and altered gait as described previously using the following system: 1, very mild deficit in hind paw gripping ability of injected foot only; 2, very mild deficit in bilateral hind paw gripping ability; 3, bilateral loss of gripping ability and mild bilateral hind limb paresis, but altered gait not readily observable; 4, bilateral loss of gripping ability, moderate bilateral hind limb paresis, observable altered gait, difficulty righting self; 5, bilateral loss of gripping ability, severe bilateral hind limb paresis, altered gait, unable to right self; 6, moribundity (29).

To determine viral titers in tissues, on the termination day of each experiment, mice were sedated with isoflurane and were euthanized by thoracotomy and exsanguination; blood was collected; and mice were perfused by intracardiac injection of 1× PBS. The right and left ankles and the right and left quadriceps muscles were removed by dissection and were weighed. Tissues were homogenized with glass beads in 1× PBS supplemented with 1% bovine calf serum, Ca^{2+}, and Mg^{2+} using a MagNA Lyser instrument (Roche) and were stored at −80°C until the amount of virus present was quantified by a standard plaque assay on BHK-21 cells.

To deplete natural killer (NK) cells, 300 μg of an anti-NK1.1 antibody (PK136 mouse IgG2a; a gift of Ron G. Gill, Department of Surgery, Uni-

versity of Colorado School of Medicine) or PBS was administered by intraperitoneal (i.p.) injection on day −1 (30).

Reverse transcription-quantitative real-time PCR (RT-qPCR). RRV RNA was quantified as described previously (29). RNA was isolated using a PureLink RNA minikit (Life Technologies). Two hundred fifty to 1,000 ng of total RNA was reverse transcribed using SuperScript III reverse transcriptase (Life Technologies). A sequence-tagged (lowercase letters) RRV-specific RT primer (starting at position 4415; 5′-ggcagtatcgtgaattcg atgcAACACTCCCGTCGACAACAGA-3′) was used for reverse transcription. A tag sequence-specific reverse primer (5′-GGCAGTATCGTGAAT TCGATGC-3′) was used with an RRV sequence-specific forward primer (starting at RRV position 4346; 5′-CCGTGGCGGGTATTATCAAT-3′) and an internal TaqMan probe (starting at RRV position 4375; 5′-ATTA AGAGTGTAGCCATCC-3′) during qPCR to enhance specificity. To create a standard curve, 10-fold-diluted RRV genomic RNA (from 10^8 to 10^0 copies), synthesized *in vitro*, was spiked into RNA from BHK-21 cells, and reverse transcription and qPCR were performed in an identical manner.

Flow cytometry. Splenocytes were incubated with anti-mouse FcγRII/FcγRIII (2.4G2; BD Pharmingen) for 20 min on ice to block nonspecific antibody binding and were then stained in fluorescence-activated cell sorting (FACS) staining buffer (1× PBS, 2% FBS) with the following antibodies from eBioscience: fluorescein isothiocyanate (FITC)-conjugated anti-CD3ε and phycoerythrin (PE)-conjugated anti-CD49b. Cells were fixed overnight in 1% paraformaldehyde, and data were acquired on an LSR II flow cytometer using FACSDiva software. FlowJo software (TreeStar) was used for all analyses.

Type I IFN ELISA and bioassay. Alpha interferon (IFN-α) and IFN-β were measured in sera by using a mouse IFN-α enzyme-linked immunosorbent assay (ELISA) (Pestka Biomedical Laboratories) (31) or a biological assay as described previously (32, 33). For the bioassay, L929 cells (ATCC CCL-1) were seeded in 96-well plates. Mouse sera and a type I IFN standard (murine IFN-α; BEI Resources), both diluted in L929 medium, were acidified to a pH of ≤2.0 for 24 h and were then neutralized to a pH of 7, treated with UV light for 10 min to inactivate residual virus, and added to cells in serial 2-fold dilutions. The following day, encephalomyocarditis virus (EMCV) was added to cells at a multiplicity of infection (MOI) of 5. Twenty-four hours later, cell viability was determined by staining monolayers with crystal violet, solubilizing the absorbed crystal violet in methanol, and measuring the absorbance at 570 nm. The type I IFN present in each sample (IU/ml) was calculated by determining the dilution of the IFN standard and of each sample that conferred 50% protection from EMCV-induced cytopathic effects. Wells that received no IFN and no EMCV served as the "cell control," the control for 100% protection. Wells that received EMCV and no IFN provided the control for 0% protection.

***In vitro* virus replication.** Triplicate wells were inoculated with virus at an MOI of 0.01. Viruses were adsorbed onto cells for 1 h at 37°C. Wells were then washed three times with 1 ml of room temperature PBS. One milliliter of growth medium was then added to each well, and cells were incubated at 37°C. For cumulative growth analysis, 100-μl samples of culture supernatants were removed at various times postinfection, and an equal volume of fresh growth medium was added to maintain a constant volume within each well. Samples were stored at −80°C for analysis by plaque assays on BHK-21 cells.

Assays of sensitivity to type I IFN. Vero cells or differentiated C2C12 cells were plated in 96-well plates or 24-well plates, respectively. The growth medium was removed, and triplicate wells were inoculated with virus at the MOIs indicated in the figure legends. Viruses were adsorbed to cells for 1 h at 37°C. Wells were then washed with three changes of room temperature 1× PBS. Growth medium was then added to each well, and cells were incubated at 37°C. At 3 h postinoculation (hpi), growth medium containing either no IFN-β or 2 to 250 IU/ml of human or murine IFN-β (BEI Resources) was added to the wells. At 48 hpi, supernatants were collected, and virus titers were determined by plaque assays on BHK-21 cells. In some experiments, Vero cells were pretreated with human IFN-β for 24 h prior to the inoculation of virus at an MOI of 5. At 24 hpi, supernatants were collected, and virus titers were determined by plaque assays on BHK-21 cells.

Statistical analysis. Viral replication and tissue titers were evaluated for statistically significant differences by using either the Student *t* test or one-way analysis of variance (ANOVA) followed by Tukey's multiple-comparison test. Disease scores were evaluated for statistically significant differences by repeated-measures ANOVA followed by Bonferroni's multiple-comparison test.

RESULTS

Coding variants in nsP1 are determinants of RRV virulence. In previous studies, we found that a chimeric virus containing the nsP1 coding region from the mouse-avirulent RRV strain DC5692 in the genetic background of the mouse-virulent strain T48 (RRV-T48-nsP1^{DC5692}) caused diminished inflammation in musculoskeletal tissues and significantly less severe musculoskeletal disease signs in mice (25). Comparison of the nsP1 coding regions of strain T48 and strain DC5692 revealed a total of 36 nucleotide differences (25). Six of these nucleotide differences are nonsynonymous and result in the following amino acid coding changes in the nsP1 sequence: S79C, A112S, L224I, C416F, S424N, and L463I. To test whether the nonsynonymous mutations were sufficient to attenuate strain T48, the six DC6592 nsP1 coding variants were introduced into the nsP1 coding region of strain T48 (RRV-T48-nsP1^{6M}) (Fig. 1A). As with RRV-T48-nsP1^{DC5692}, which contains the complete DC5692 nsP1 coding region in the T48 strain genetic background (Fig. 1A), inoculation of mice with RRV-T48-nsP1^{6M} (Fig. 1A) resulted in significantly less severe disease signs (Fig. 1B [P, <0.01 for RRV T48 versus RRV-T48-nsP1^{DC5692} and <0.05 for RRV T48 versus RRV-T48-nsP1^{6M}] and C). These findings indicated that the six nonsynonymous mutations in nsP1 derived from strain DC5692 are sufficient for the attenuated phenotype. We next tested whether replacement of the six nsP1 coding variants in strain DC5692 with the nonsynonymous nucleotides from strain T48 would result in a gain of virulence. As reported previously, replacement of the strain DC5692 nsP1 and PE2 coding regions with those from strain T48 was required to confer full virulence on the mouse-avirulent strain DC5692 (25). Thus, we introduced the six T48 nsP1 coding variants into a chimeric RRV genome that carries the T48 PE2 coding region in the genetic background of strain DC5692 (RRV-DC5692-PE2^{T48}) to generate RRV-DC5692-nsP1^{6M}-PE2^{T48} (Fig. 1A). In agreement with previously reported findings (25), inoculation of mice with RRV-DC5692-PE2^{T48} (previously referred to as RR108) resulted in significantly less severe disease signs in mice (Fig. 1D and E). In contrast, inoculation of mice with RRV-DC5692-nsP1^{6M}-PE2^{T48} resulted in disease signs and tissue pathology that were indistinguishable from those for RRV T48-inoculated mice (Fig. 1D and E).

To investigate whether the attenuated phenotype of RRV-T48-nsP1^{6M} in WT mice was associated with differences in viral loads in tissues, mice were inoculated with RRV T48 or RRV-T48-nsP1^{6M}, and the amounts of infectious virus present in serum, ankle/foot tissues, and quadriceps muscle tissues at 1, 3, 5, and 7 dpi were quantified by plaque assays (Fig. 2). In agreement with our previously published studies finding that viral loads in mice inoculated with RRV T48 or RRV-T48-nsP1^{DC5692} were similar (25), the amounts of infectious virus in the sera (Fig. 2A), ankles/feet (Fig. 2B and C), and quadriceps muscles (Fig. 2D and E) of RRV T48-inoculated mice at 1, 3, and 5 dpi did not generally

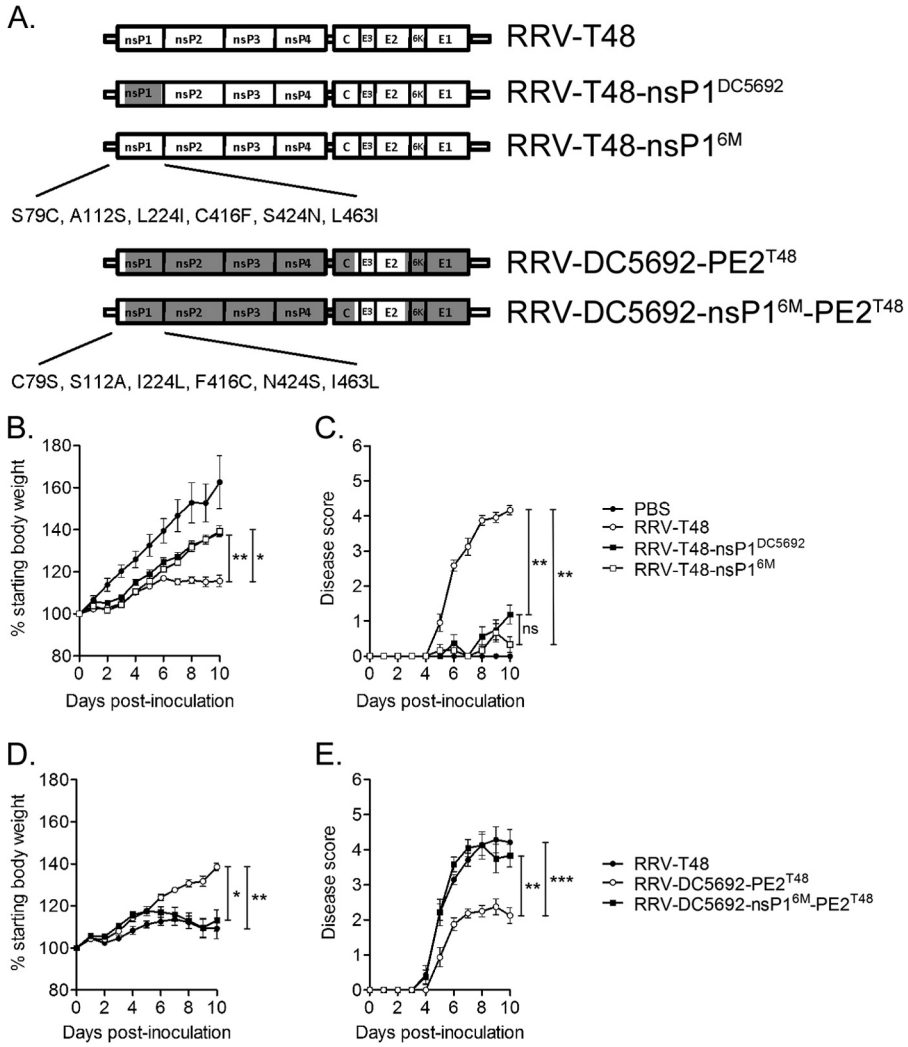

FIG 1 Coding variants in nsP1 are determinants of RRV virulence. (A) Schematic representations of the genomes of the Ross River viruses used in this study. Open rectangles, sequences derived from the mouse-virulent strain T48; shaded rectangles, sequences derived from the mouse-avirulent strain DC5692. (B and C) Three- to 4-week-old C57BL/6 mice were inoculated either with PBS ($n = 7$) or with 10^3 PFU of RRV T48 ($n = 12$), RRV-T48-nsP1^{DC5692} ($n = 8$), or RRV-T48-nsP1^{6M} ($n = 9$) by injection in the left rear footpad. At 24-h intervals, mice were assessed for weight gain (B) and were scored for musculoskeletal disease signs, including loss of gripping ability and altered gait (C). Each data point represents the arithmetic mean ± standard error of the mean. Data were evaluated for statistically significant differences by a repeated-measures ANOVA followed by Bonferroni's multiple-comparison test. *, $P < 0.05$; **, $P < 0.01$. (D and E) Three- to 4-week-old C57BL/6 mice were inoculated with 10^3 PFU of RRV T48 ($n = 7$), RRV-DC5692-PE2^{T48} ($n = 8$), or RRV-DC5692-nsP1^{6M}-PE2^{T48} ($n = 11$) by injection in the left rear footpad. At 24-h intervals, mice were assessed for weight gain (D) and were scored for musculoskeletal disease signs, including loss of gripping ability and altered gait (E). Each data point represents the arithmetic mean ± standard error of the mean. Data were evaluated for statistically significant differences by a repeated-measures ANOVA followed by Bonferroni's multiple-comparison test. *, $P < 0.05$; **, $P < 0.01$; ***, $P < 0.001$.

exceed those for RRV-T48-nsP1^{6M}-inoculated mice. At 7 dpi, the titers of RRV-T48-nsP1^{6M} in both the left and right ankles were significantly lower than those of RRV T48 (9.8-fold [P, <0.001] and 5.1-fold [P, <0.05], respectively) (Fig. 2B and C).

RRV-T48-nsP1^{6M} is attenuated in *Rag1*$^{-/-}$ mice. Our experiments with WT mice indicated that RRV-T48-nsP1^{6M} had an impact on weight gain (relative to the weight gain of mock-infected mice) similar to that of the virulent strain RRV T48 from days 1 to 6 postinoculation (Fig. 1B). From 6 to 10 dpi, mice inoculated with RRV-T48-nsP1^{6M} continued to gain weight at a rate similar to that of mock-infected mice, consistent with the minimal musculoskeletal disease signs (Fig. 1C), whereas mice inoculated with RRV T48 showed significantly reduced weight gain during this time frame (Fig. 1B). In addition, the viral loads in the tissues of WT mice inoculated with these viruses were similar until 7 dpi (Fig. 2). On the basis of these data, we hypothesized that RRV-T48-nsP1^{6M} is more susceptible to some aspect of the adaptive immune response, which typically arises at ~1 week postvirus infection. To test this hypothesis, *Rag1*$^{-/-}$ C57BL/6 mice, which lack mature T and B lymphocytes due to an inability to perform V(D)J recombination of immunoglobulin and T cell receptor genes (34), were inoculated with RRV T48 or RRV-T48-nsP1^{6M} and were monitored for the development of disease signs. As shown in Fig. 3A and B, inoculation of *Rag1*$^{-/-}$ mice with RRV-T48-nsP1^{6M} resulted in disease signs significantly less severe than those of *Rag1*$^{-/-}$ mice inoculated with RRV T48.

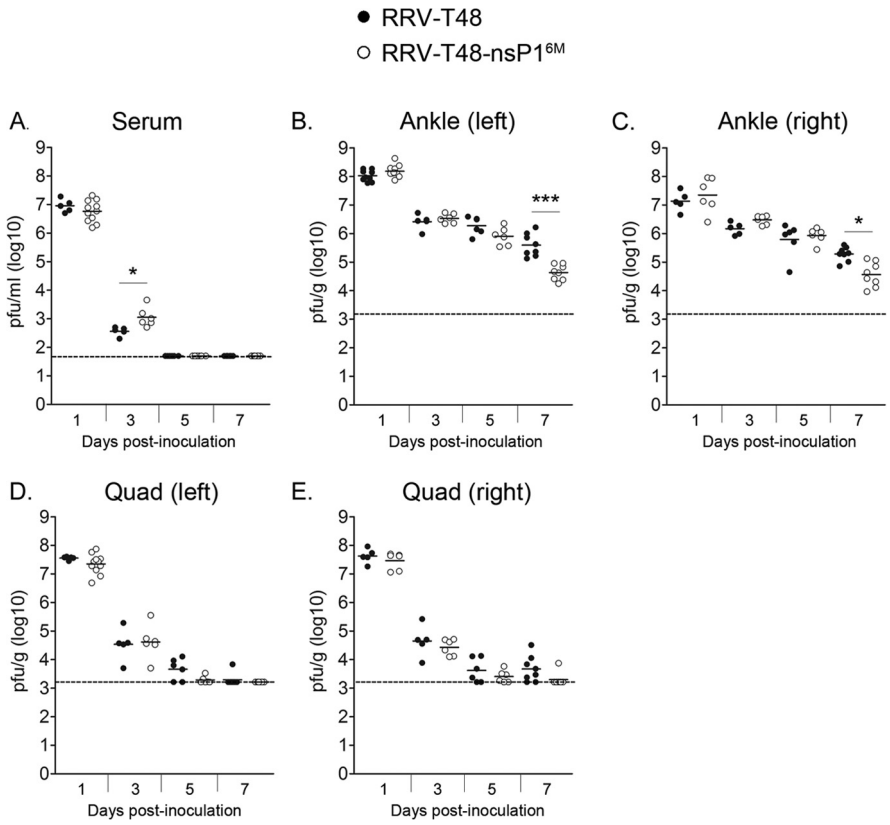

FIG 2 Infectious virus in tissues of WT mice. Three- to 4-week-old C57BL/6 mice were inoculated with 10^3 PFU of RRV T48 (filled circles) or RRV-T48-nsP1^{6M} (open circles) by injection in the left rear footpad. At 1, 3, 5, and 7 dpi, mice (n, 5 to 11) were sacrificed, blood was collected via cardiac puncture, and mice were perfused by intracardial injection with 1× PBS. Tissues were dissected, weighed, and homogenized, and the amounts of infectious virus present in the serum (A), left ankle/foot (B), right ankle/foot (C), left quadriceps muscle (D), and right quadriceps muscle (E) of each mouse were quantified by plaque assays on BHK-21 cells. Dashed lines indicate the limits of detection. Asterisks indicate significant differences (*, $P < 0.05$; ***, $P < 0.001$) as determined by ANOVA followed by Tukey's multiple-comparison test.

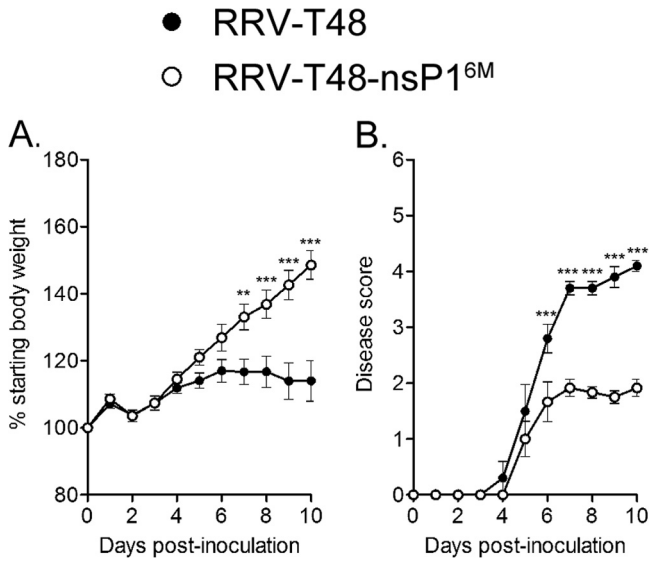

FIG 3 RRV-T48-nsP1^{6M} is attenuated in *Rag1*$^{-/-}$ mice. Three- to 4-week-old *Rag1*$^{-/-}$ C57BL/6 mice were inoculated with 10^3 PFU of RRV T48 ($n = 5$) or RRV-T48-nsP1^{6M} ($n = 6$) by injection in the left rear footpad. At 24-h intervals, mice were assessed for weight gain (A) and were scored for musculoskeletal disease signs, including loss of gripping ability and altered gait (B). Each data point represents the arithmetic mean ± standard error of the mean. Data were evaluated for statistically significant differences by a repeated-measures ANOVA followed by Bonferroni's multiple-comparison test. **, $P < 0.01$; ***, $P < 0.001$.

To investigate whether the attenuated phenotype of RRV-T48-nsP1^{6M} in *Rag1*$^{-/-}$ mice was associated with differences in viral loads in tissues, *Rag1*$^{-/-}$ mice were inoculated with RRV T48 or RRV-T48-nsP1^{6M}, and the amounts of infectious virus present in sera, ankle/foot tissues, and quadriceps muscle tissues at 1, 3, 5, and 7 dpi were quantified by plaque assays (Fig. 4). The titers of RRV-T48-nsP1^{6M} in sera were significantly higher than the titers of RRV T48 at 3 dpi (4.8-fold [P, <0.01]) and 5 dpi (8.6-fold [P, <0.001]) (Fig. 4A). In contrast to the findings for WT mice, no differences in viral titers were detected in ankle/foot tissues at the time points analyzed (Fig. 4B and C). The titers of RRV-T48-nsP1^{6M} in both the left and right quadriceps muscle tissues were similar to those of RRV T48 at 1 and 3 dpi (Fig. 4D and E). However, by 5 dpi, the titers of RRV-T48-nsP1^{6M} in both the left and right quadriceps muscle tissues were significantly lower than those of RRV T48 (7-fold [P, <0.01] and 6.2-fold [P, <0.01], respectively). By 7 dpi, the differences in the viral titers in the left and right quadriceps muscles were more dramatic (54-fold [P, <0.001] and 10.2-fold [P, <0.001], respectively). In fact, at 7 dpi, infectious virus was detectable in 14 of 14 quadriceps muscles of mice inoculated with RRV T48, whereas only 2 of 14 quadriceps muscles of mice inoculated with RRV-T48-nsP1^{6M} had detectable infectious virus (Fig. 4D and E).

To confirm these data, we quantified the RRV RNA present in the right quadriceps muscles of RRV T48- and RRV-T48-nsP1^{6M}-

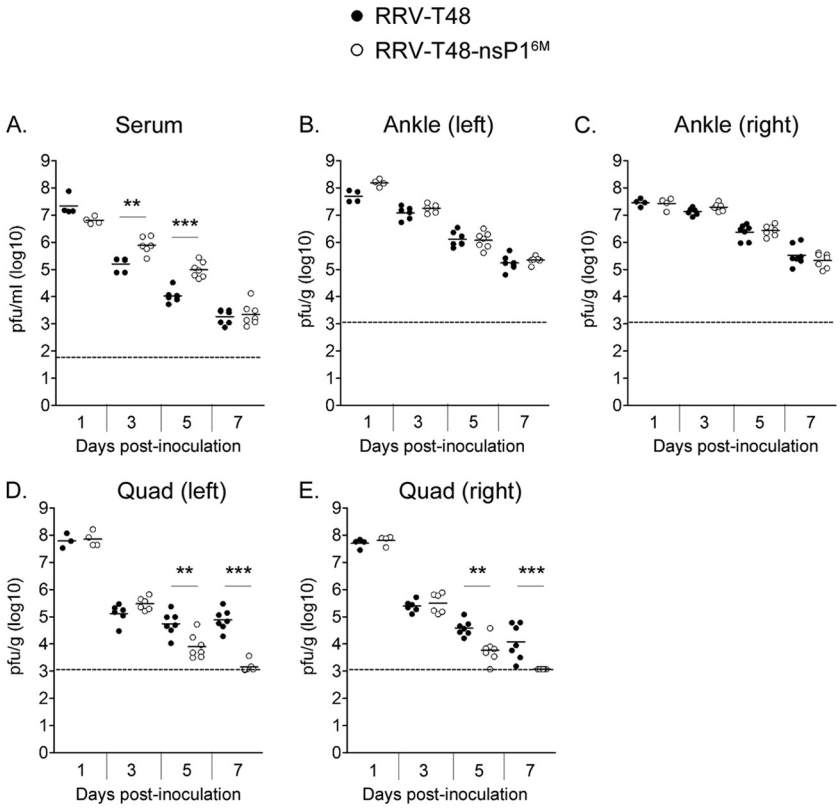

FIG 4 Infectious virus in tissues of *Rag1*$^{-/-}$ mice. (A to E) Three- to 4-week-old *Rag1*$^{-/-}$ C57BL/6 mice were inoculated with 10^3 PFU of RRV T48 (filled circles) or RRV-T48-nsP1^{6M} (open circles) by injection in the left rear footpad. At 1, 3, 5, and 7 dpi, mice (*n*, 4 to 7) were sacrificed, blood was collected via cardiac puncture, and mice were perfused by intracardial injection with 1× PBS. Tissues were dissected, weighed, and homogenized, and the amounts of infectious virus present in the serum (A), left ankle/foot (B), right ankle/foot (C), left quadriceps muscle (D), and right quadriceps muscle (E) of each mouse were quantified by plaque assays on BHK-21 cells. Dashed lines indicate the limits of detection. Asterisks indicate significant differences (**, $P < 0.01$; ***, $P < 0.001$) as determined by ANOVA followed by Tukey's multiple-comparison test.

infected *Rag1*$^{-/-}$ mice at 3, 5, and 7 dpi by real-time RT-qPCR. At 3 dpi, we detected a small but significant increase in the level of RRV RNA in the right quadriceps muscles of mice inoculated with RRV-T48-nsP1^{6M} (2.5-fold [*P*, <0.01]) (Fig. 5A). However, at both 5 and 7 dpi, RRV RNA levels in the right quadriceps were dramatically lower in RRV-T48-nsP1^{6M}-infected mice than in RRV T48-infected mice (22.8-fold [*P*, <0.001] and 71.8-fold [*P*, <0.001], respectively) (Fig. 5A). The differences in RNA levels were similar whether we calculated the quantity of RRV genomes per microgram of RNA (Fig. 5A) or per gram of tissue (data not shown). To explore whether our analysis of infectious virus present in quadriceps muscle tissues of WT mice was misleading due to the potential presence of antiviral antibodies and/or the fact that titers at 5 and 7 dpi were near or below the limit of detection (Fig. 2D and E), we quantified the RRV RNA present in the right quadriceps muscles of RRV T48- and RRV-T48-nsP1^{6M}-infected WT mice at 3, 5, and 7 dpi. As with *Rag1*$^{-/-}$ mice, the levels of RRV RNA were similar at 3 dpi but dramatically reduced in mice inoculated with RRV-T48-nsP1^{6M} at both 5 and 7 dpi (91.2-fold [*P*, <0.001] and 30-fold [*P*, <0.001], respectively) (Fig. 5B). In contrast, at 7 dpi, the levels of RRV RNA in the left (Fig. 5C) and right (Fig. 5D) ankles of WT mice inoculated with RRV T48 or RRV-T48-nsP1^{6M} were similar. Taken together, our findings for WT and *Rag1*$^{-/-}$ mice suggest that the attenuating mutations in nsP1 of RRV-T48-nsP1^{6M} render the virus more susceptible to tissue-specific host antiviral responses.

Depletion of NK cells or deletion of IFN-γ does not rescue RRV-T48-nsP1^{6M} loads in skeletal muscle tissue. The timing of the differences in the loads of RRV T48 and RRV-T48-nsP1^{6M} in the skeletal muscle tissue of WT and *Rag1*$^{-/-}$ mice (Fig. 4 and 5) correlated with the infiltration of this tissue with natural killer (NK) cells and macrophages (15). To test if the reduced loads of RRV-T48-nsP1^{6M} in skeletal muscle tissue were due to the antiviral activity of NK cells, 300 μg of an anti-NK1.1 monoclonal antibody was administered intraperitoneally to WT (Fig. 6A to C) or *Rag1*$^{-/-}$ (Fig. 6D to F) mice 1 day before inoculation with RRV-T48-nsP1^{6M}. At 5 dpi, the levels of RRV-T48-nsP1^{6M} RNA present in the right quadriceps muscles of WT (Fig. 6A) or *Rag1*$^{-/-}$ (Fig. 6D) mice treated with the anti-NK1.1 antibody were similar to those in PBS-injected control mice. In addition, the RRV-T48-nsP1^{6M} RNA levels in WT and *Rag1*$^{-/-}$ mice treated with the anti-NK1.1 antibody were similar to those detected in untreated RRV-T48-nsP1^{6M}-infected mice and remained dramatically lower than the RRV RNA levels in skeletal muscle tissues of RRV T48-infected mice (Fig. 6A and D; graphed from Fig. 5 for comparison). Flow cytometric analysis of splenocytes harvested at 5 dpi from WT (Fig. 6B and C) or *Rag1*$^{-/-}$ (Fig. 6E and F) mice confirmed that administration of the anti-NK1.1 antibody significantly reduced the number of CD3$^-$ CD49b$^+$ NK cells. The production of IFN-γ by NK cells and other cell types contributes to antiviral defense (35). To evaluate if the reduced loads of RRV-T48-nsP1^{6M} in skeletal muscle tissue were due to the effects of

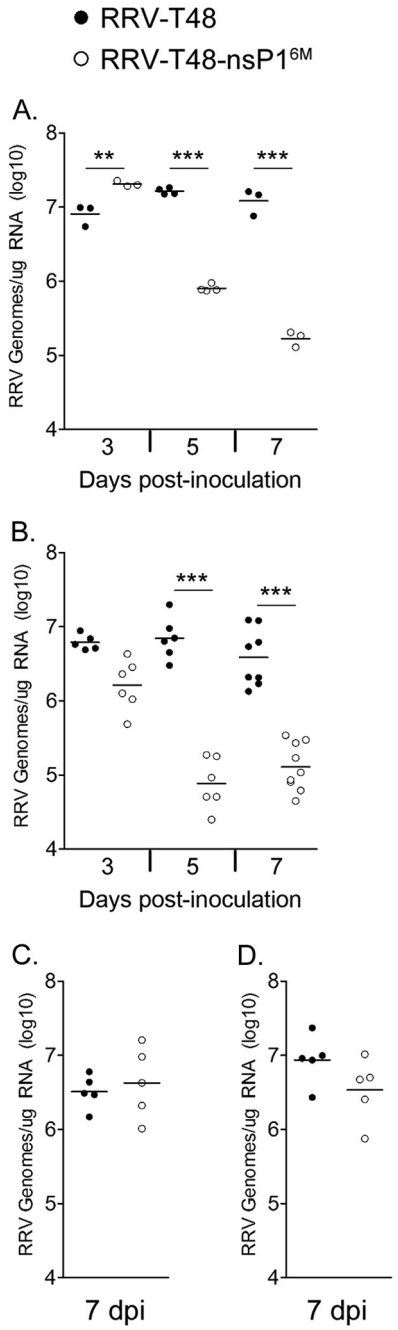

FIG 5 RRV RNA levels in tissues of *Rag1*$^{-/-}$ and WT mice. Three- to 4-week-old *Rag1*$^{-/-}$ (A) or WT (B to D) C57BL/6 mice were inoculated with 10^3 PFU of RRV T48 (filled circles) or RRV-T48-nsP1^{6M} (open circles) by injection in the left rear footpad. At 3, 5, and 7 dpi, mice were sacrificed and were perfused by intracardial injection with 1× PBS, and total RNA was isolated from the right quadriceps muscles (A and B), the left ankle (C), and the right ankle (D). RRV genomic RNA was quantified by RT-qPCR. Horizontal bars indicate means, and dashed lines indicate the limits of detection. Asterisks indicate significant differences (**, $P < 0.01$; ***, $P \leq 0.001$) as determined by ANOVA followed by Tukey's multiple-comparison test.

IFN-γ, we inoculated C57BL/6 mice deficient in IFN-γ (*Ifng*$^{-/-}$) with RRV T48 or RRV-T48-nsP1^{6M} and quantified the RRV RNA present in the right quadriceps muscles at 5 dpi by real-time RT-qPCR. As with WT and *Rag1*$^{-/-}$ mice, RRV RNA levels in the right quadriceps were dramatically lower in RRV-T48-nsP1^{6M}-infected *Ifng*$^{-/-}$ mice than in RRV T48-infected *Ifng*$^{-/-}$ mice (328-fold [P, <0.0001]) (Fig. 6G). Taken together, these data suggest that the attenuating mutations in nsP1 of RRV-T48-nsP1^{6M} do not render the virus more susceptible to NK cell-mediated clearance or to the antiviral effects of IFN-γ.

Attenuating mutations in nsP1 enhance sensitivity to type I IFN. Overall, our analyses revealed that the attenuating mutations in nsP1 enhanced host control of RRV infection in skeletal muscle tissues, but not in ankle/foot tissues or sera, of WT and *Rag1*$^{-/-}$ mice, suggesting that RRV-T48-nsP1^{6M} is more susceptible to some aspect of the host's innate antiviral response in skeletal muscle tissues and likely explaining the attenuated disease signs. However, depletion of NK cells or genetic deletion of IFN-γ failed to rescue loads of the nsP1 mutant virus in skeletal muscle tissue. Type I IFN is a component of the host's innate antiviral response and a critical regulator of alphavirus replication, spread, and virulence (36). To test whether RRV T48 and RRV-T48-nsP1^{6M} are equally virulent in the absence of the effects of type I interferon, we inoculated *Ifnar1*$^{-/-}$ C57BL/6 mice with 1,000 PFU of RRV T48 or RRV-T48-nsP1^{6M} and monitored the mice for survival. As shown in Fig. 7A, RRV T48 and RRV-T48-nsP1^{6M} were equally virulent in 3- to 4-week-old *Ifnar1*$^{-/-}$ mice; all mice were moribund by 40 to 44 h postinoculation. Due to the rapid time to morbidity in mice of this age, we were unable to evaluate viral loads in quadriceps muscle tissue at later times postinoculation. To that end, we tested the extent to which inoculation of older *Ifnar1*$^{-/-}$ mice with lower doses of virus would increase survival time. We found that inoculation of 12- to 14-week-old *Ifnar1*$^{-/-}$ mice with 5 PFU of virus extended the time to morbidity until 4 dpi. As shown in Fig. 7B, RRV RNA levels in the left and right quadriceps of *Ifnar1*$^{-/-}$ mice at 4 dpi were slightly lower in RRV-T48-nsP1^{6M}-infected mice than in RRV T48-infected mice (4-fold and 6-fold, respectively); however, these differences were not statistically significant. Although it remains possible that these differences in viral loads would be exacerbated at 5 dpi, taken together, our data suggest that the attenuating mutations in nsP1 of RRV-T48-nsP1^{6M} render the virus more susceptible to the type I IFN response in skeletal muscle tissue.

We next investigated if RRV-T48-nsP1^{6M} is a more potent inducer of type I IFN and/or is more sensitive to antiviral effector functions activated by type I IFN. At 24 hpi, despite equivalent viral loads in sera and other tissues (Fig. 2), we detected significantly more IFN-α in the sera of RRV T48-infected WT mice than in the sera of RRV-T48-nsP1^{6M}-infected WT mice (Fig. 7C) (P, <0.001). However, at 12, 48, 72, and 120 hpi, similar levels of systemic IFN-α were detected in the sera of RRV T48-infected and RRV-T48-nsP1^{6M}-infected WT mice (Fig. 7C). Similar results were observed at 48 hpi by use of a type I IFN bioassay (data not shown). These data suggest that the attenuated phenotype of RRV-T48-nsP1^{6M} is not due to enhanced induction of systemic type I interferon.

In vitro, virus yields from Vero cells and differentiated C2C12 murine muscle cells inoculated with RRV T48 or RRV-T48-nsP1^{6M} at a low MOI (0.01) were similar at 6, 12, 24, and 48 hpi (Fig. 8A and B), indicating that these two cell lines could be utilized to test the effects of exogenous IFN on virus replication. To test whether RRV-T48-nsP1^{6M} is more sensitive to type I IFN, Vero cells, which respond to type I IFN but cannot produce type I IFN (37, 38), were inoculated with RRV T48 or RRV-T48-nsP1^{6M}

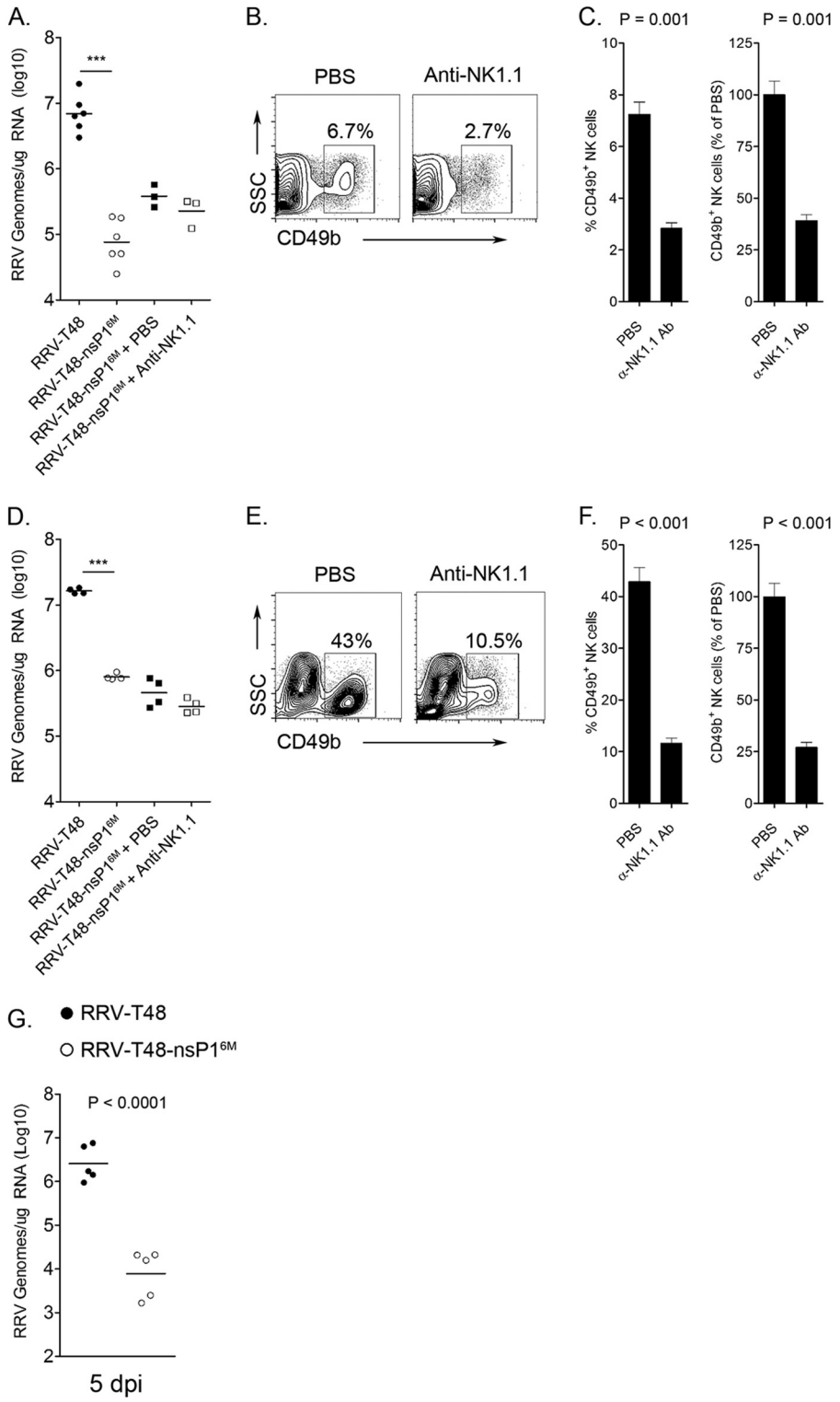

FIG 6 Depletion of NK cells or deletion of IFN-γ fails to restore RRV-T48-nsP1^{6M} loads in skeletal muscle tissue. (A to F) Three- to 4-week-old WT (A to C) or *Rag1*$^{-/-}$ (D to F) C57BL/6 mice were injected i.p. with PBS or 300 μg of an anti-NK1.1 antibody on day −1. On day zero, mice were inoculated with 10^3 PFU of RRV-T48-nsP1^{6M} by injection in the left rear footpad. (A and D) At 5 dpi, WT (A) or *Rag1*$^{-/-}$ (D) mice were sacrificed and were perfused with PBS via intracardiac injection with 1× PBS, and RRV RNA in the right quadriceps muscle was quantified by RT-qPCR. Levels of RRV RNA in untreated mice infected with RRV T48 or RRV-T48-nsP1^{6M} were graphed for comparison. Horizontal bars indicate means. Asterisks indicate significant differences (***, $P \leq 0.001$) as determined by ANOVA followed by Tukey's multiple-comparison test. (B and E) Total splenocytes from WT (B) and *Rag1*$^{-/-}$ (E) mice were analyzed by flow cytometry for the expression of CD49b. Representative contour plots are shown. SSC, side scatter. (C and F) Percentages of CD49b$^+$ cells in the spleens of WT (C) and *Rag1*$^{-/-}$ (F) mice. Each bar represents the arithmetic mean ± standard error of the mean. *P* values were determined using two-tailed unpaired *t* tests. (G) Three- to 4-week-old *Ifng*$^{-/-}$ C57BL/6 mice were inoculated with 10^3 PFU of RRV T48 or RRV-T48-nsP1^{6M} by injection in the left rear footpad. At 5 dpi, mice were sacrificed and were perfused with PBS via intracardiac injection with 1× PBS, and RRV RNA in the right quadriceps muscle was quantified by RT-qPCR. Horizontal bars indicate means. The *P* value was determined by a two-tailed unpaired *t* test.

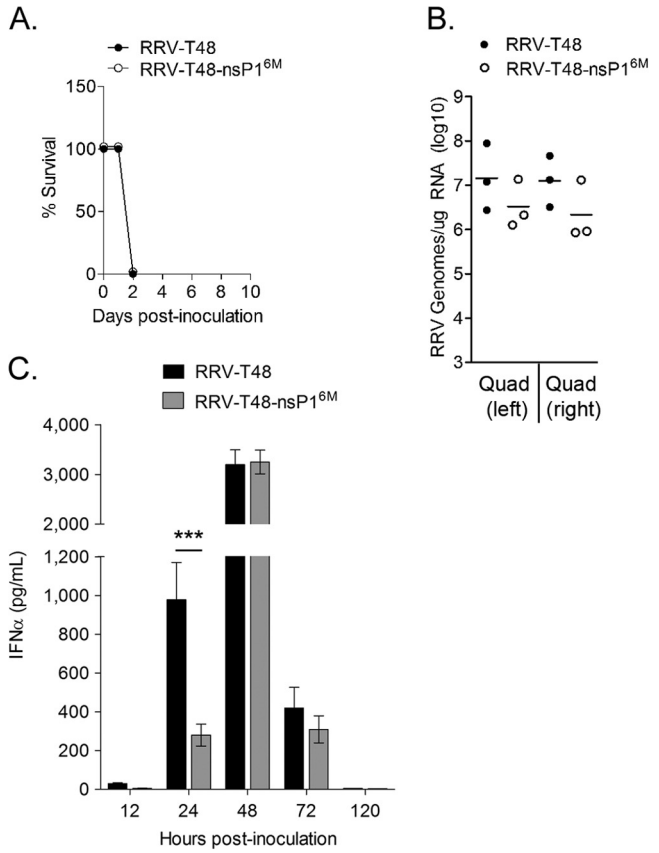

FIG 7 Virulence and RRV RNA levels in *Ifnar1*$^{-/-}$ mice. (A) Three- to 4-week-old *Ifnar1*$^{-/-}$ C57BL/6 mice were inoculated with 10^3 PFU of RRV T48 (filled circles) or RRV-T48-nsP1^{6M} (open circles) by injection in the left rear footpad, and mice were monitored for survival. (B) Twelve- to 14-week-old *Ifnar1*$^{-/-}$ C57BL/6 mice were inoculated with 5 PFU of RRV T48 (filled circles) or RRV-T48-nsP1^{6M} (open circles) by injection in the left rear footpad. At 4 dpi, mice were sacrificed and were perfused by intracardial injection with 1× PBS, and RRV genomic RNA in the quadriceps muscles was quantified by RT-qPCR. Horizontal bars indicate means. No statistically significant differences were detected by two-tailed unpaired *t* tests. (C) Three- to 4-week-old WT C57BL/6 mice were either mock inoculated or inoculated with 10^3 PFU of RRV T48 or RRV-T48-nsP1^{6M} by injection in the left rear footpad. At 12 (*n*, 5 mice/group), 24 (*n*, 4 to 5 mice/group), 48 (*n*, 4 mice/group), 72 (*n*, 7 to 8 mice/group), and 120 (*n*, 10 mice/group) hpi, mice were sacrificed, blood was collected via cardiac puncture, and the amount of IFN-α was quantified by ELISA.

at a low MOI (0.1 PFU/cell). At 3 hpi, cells either were mock treated or were treated with various amounts of IFN-β, and virus yields in the culture supernatants at 48 hpi were quantified by plaque assays. As shown in Fig. 8C, RRV-T48-nsP1^{6M} showed higher sensitivity to IFN-β treatment than RRV T48 (19.5-fold and 295-fold decreases in virus yields at 16 IU/ml and 32 IU/ml of IFN-β, respectively [*P*, <0.05 and <0.001, respectively]). Similarly, RRV-T48-nsP1^{6M} showed higher sensitivity to IFN-β treatment than RRV T48 in differentiated C2C12 murine myoblasts (Fig. 8D) (8.5-fold and 42-fold decreases in virus yields at 50 IU/ml and 250 IU/ml IFN-β, respectively [*P*, <0.001]). RRV-T48-nsP1^{6M} also showed increased sensitivity to IFN-β when Vero cells were pretreated with IFN-β for 24 h and were then inoculated at a high MOI (5 PFU/cell) (6-fold decrease at 32 IU/ml IFN-β [*P*, <0.05]) (Fig. 8E). Overall, the attenuating mutations in nsP1 appear to enhance the sensitivity of RRV to type I IFN *in vitro*, and RRV-T48-nsP1^{6M} virulence and loads in skeletal muscle tissue are restored *in vivo* in mice unable to respond to type I IFN.

The attenuated phenotype requires two nsP1 coding changes. To determine whether the attenuated phenotype of RRV-T48-nsP1^{6M} could be attributed to a single coding change, each nonsynonymous mutation found in RRV DC5692 nsP1 was individually introduced into the cDNA clone of strain RRV T48, and the abilities of viruses derived from these clones to cause disease in the mouse model were tested. As shown in Fig. 9A and B, inoculation of groups of WT mice with 10^3 PFU of each virus revealed that no single mutation fully recapitulated the attenuated phenotype observed in WT mice inoculated with RRV-T48-nsP1^{6M} (Fig. 1B and C). However, mice inoculated with either RRV-T48-nsP1-S79C or RRV-T48-nsP1-L224I developed significantly milder disease signs than mice inoculated with RRV T48 (Fig. 9B). Therefore, we constructed a double mutant virus carrying both of these mutations in nsP1. Both by weight gain measurements (Fig. 9C) and by scoring of musculoskeletal disease signs (Fig. 9D), RRV-T48-nsP1-S79C;L224I was attenuated in WT mice to a similar level as RRV-T48-nsP1^{6M}, suggesting that these two DC5692 nsP1 coding variants are sufficient for the attenuated phenotype.

Our experiments with RRV-T48-nsP1^{6M} suggested that the attenuated phenotype in mice may be due to increased sensitivity to type I IFN (Fig. 8). To investigate if RRV-T48-nsP1-S79C;L224I also has enhanced sensitivity to type I IFN, we compared the type I IFN sensitivity of RRV-T48-nsP1-S79C;L224I to those of both RRV T48 and RRV-T48-nsP1^{6M} in Vero cells. As shown in Fig. 9E, RRV-T48-nsP1^{6M} and RRV-T48-nsP1-S79C;L224I showed higher sensitivity to IFN-β treatment than RRV T48 (234-fold, 98-fold, and 18.2-fold decreases in virus yields at 32 IU/ml of IFN-β, respectively *P*, <0.001 and <0.01, respectively).

DISCUSSION

Identification of virulence determinants within nsP1. To determine which of the nucleotide differences in nsP1 between RRV T48 and DC5692 were responsible for the attenuated disease phenotype of RRV-T48-NSP1^{DC5692} (25), we introduced the six DC5692 nsP1 coding variants into the mouse-virulent RRV T48 genome to create RRV-T48-nsP1^{6M}. We found that, in comparison to infection with RRV T48, RRV-T48-nsP1^{DC5692} and RRV-T48-nsP1^{6M} were equally attenuated in the mouse model, indicating that the six coding changes within the nsP1 sequence were sufficient for the attenuated phenotype. Furthermore, introduction of the six RRV T48 nsP1 coding variants into the attenuated RRV-DC5692-PE2^{T48} strain resulted in a gain of virulence, confirming that these nsP1 mutations are determinants of RRV virulence. Introduction of the six DC5692 nsP1 coding variants individually into the RRV T48 genetic background failed to reproduce the attenuated phenotype of RRV-T48-nsP1^{6M}, indicating that attenuation was not due to a single point mutation. However, the disease signs in mice inoculated with either RRV-T48-nsP1-S79C or RRV-T48-nsP1-L224I were significantly less severe than those in RRV T48-infected mice. Thus, we generated a mutant virus containing both these mutations (RRV-T48-nsP1-S79C;L224I) and observed an attenuated phenotype similar to that of RRV T48-nsP1^{6M}, indicating that these are the major attenuating mutations within nsP1.

The nsP1 protein of alphaviruses is a replicase protein of 534 to 540 amino acids that functions in viral RNA replication and viral

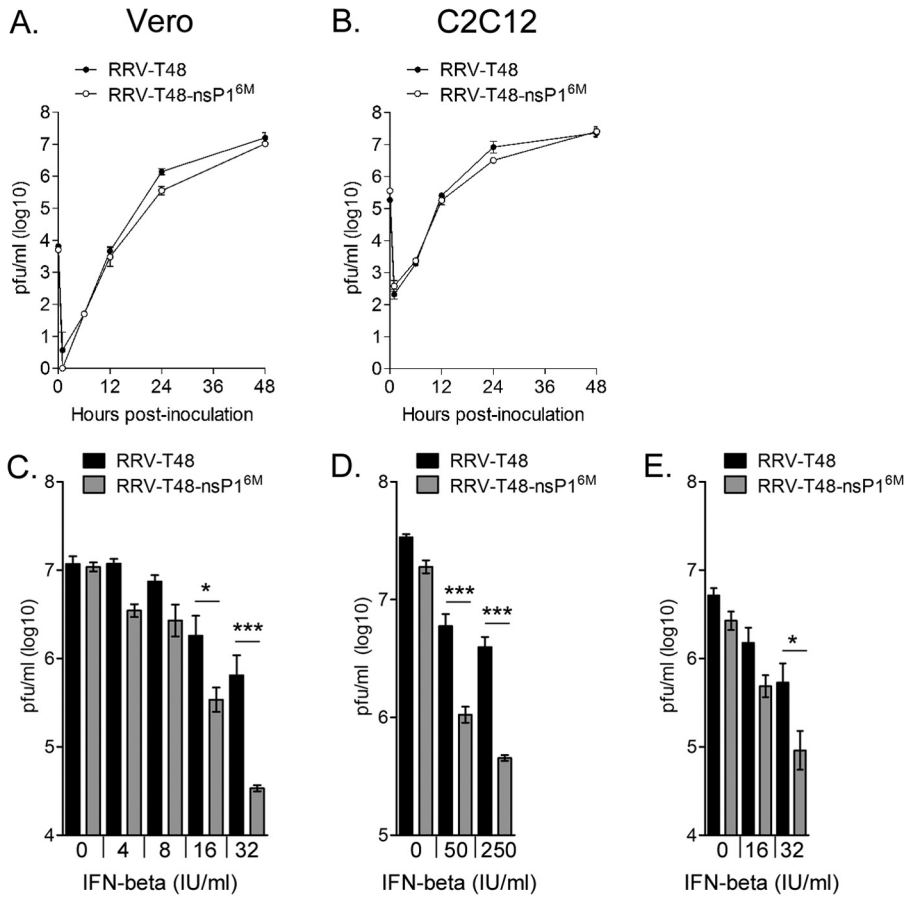

FIG 8 Attenuating mutations in nsP1 enhance the sensitivity of RRV to type I IFN. (A and B) Vero cells (A) or differentiated C2C12 murine muscle cells (B) were inoculated with RRV T48 or RRV-T48-nsP1^{6M} at an MOI of 0.01. At 0 hpi (input) and 12, 24, and 48 hpi, the amounts of infectious virus present in culture supernatants were quantified by plaque assays. (C) Virus yields at 48 hpi in Vero cells treated with increasing doses of IFN-β 3 h after infection with RRV T48 or RRV-T48-nsP1^{6M} (MOI, 0.1). Asterisks indicate significant differences (*, $P < 0.05$; ***, $P < 0.001$) as determined by ANOVA followed by Tukey's multiple-comparison test. (D) Virus yields at 48 hpi in differentiated C2C12 cells treated with increasing doses of IFN-β 3 h after infection with RRV T48 or RRV-T48-nsP1^{6M} (MOI, 1). Asterisks indicate significant differences (***, $P < 0.001$) as determined by ANOVA followed by Tukey's multiple-comparison test. (E) Virus yields at 24 hpi in Vero cells treated with increasing doses of IFN-β 24 h prior to infection with RRV T48 or RRV-T48-nsP1^{6M} (MOI, 5). The asterisk indicates a significant difference (*, $P < 0.05$) as determined by ANOVA followed by Tukey's multiple-comparison test.

RNA capping (39). The capping activities of nsP1 are essential for viral replication (40). The structure of nsP1 is unknown, and studies have failed to define specific enzymatic subdomains. Analysis of purified recombinant nsP1 by circular dichroism revealed that a high percentage of nsP1 residues are in disordered regions and not in the regular secondary structure (41). It was postulated that these disordered regions may participate in specific interactions with other proteins, nucleic acids, or membranes (41). Due to the lack of information regarding the structure of nsP1, the roles of amino acid positions 79 and 224 in nsP1 structure-function are unclear. Amino acid sequence alignments of nsP1 proteins of alphaviruses in the Semliki Forest antigenic complex, which includes RRV, CHIKV, Semliki Forest virus (SFV), Mayaro virus, and o'nyong-nyong virus, revealed that positions 79 and 224 are in highly conserved regions of the nsP1 sequence (see Table S1 in the supplemental material). In all sequences analyzed, a cysteine was present at position 79, including two entries for the RRV T48 sequence (GenBank accession no. GQ433359 and DQ226993). However, the RRV T48 sequence encoded in the pRR64 plasmid, which was generated from RRV T48 obtained from the Yale Arbovirus Research Unit (26), has a serine at nsP1 position 79, suggesting that this mutation may be the result of repeated passages in mice prior to cDNA cloning of the viral genome (26, 27). Except in RRV strains DC5692 (GenBank accession no. HM234643) and NB5092 (GenBank accession no. M20162), all nsP1 sequences analyzed have a leucine at nsP1 position 224. Like RRV DC5692, RRV NB5092 has an isoleucine at nsP1 position 224 and is attenuated in mice (25, 42).

In studies of temperature-sensitive (*ts*) mutants of SFV and Sindbis virus (SINV), only three *ts* mutations (D119N, E529D, and A348T), have been mapped to nsP1. Each of these mutants is specifically defective in minus-strand RNA synthesis, demonstrating an important role for nsP1 in RNA replication (43, 44). Although the three *ts* mutations of nsP1 cause similar defects in minus-strand synthesis, they are located in different parts of the primary sequence of the protein (43). The nsP1 protein also has guanine-7-methyltransferase and guanylyltransferase activities, which are essential for capping and cap methylation of viral RNAs by mechanisms that are distinct from host RNA-capping mechanisms (45–48). The N terminus of nsP1 is predicted to function as

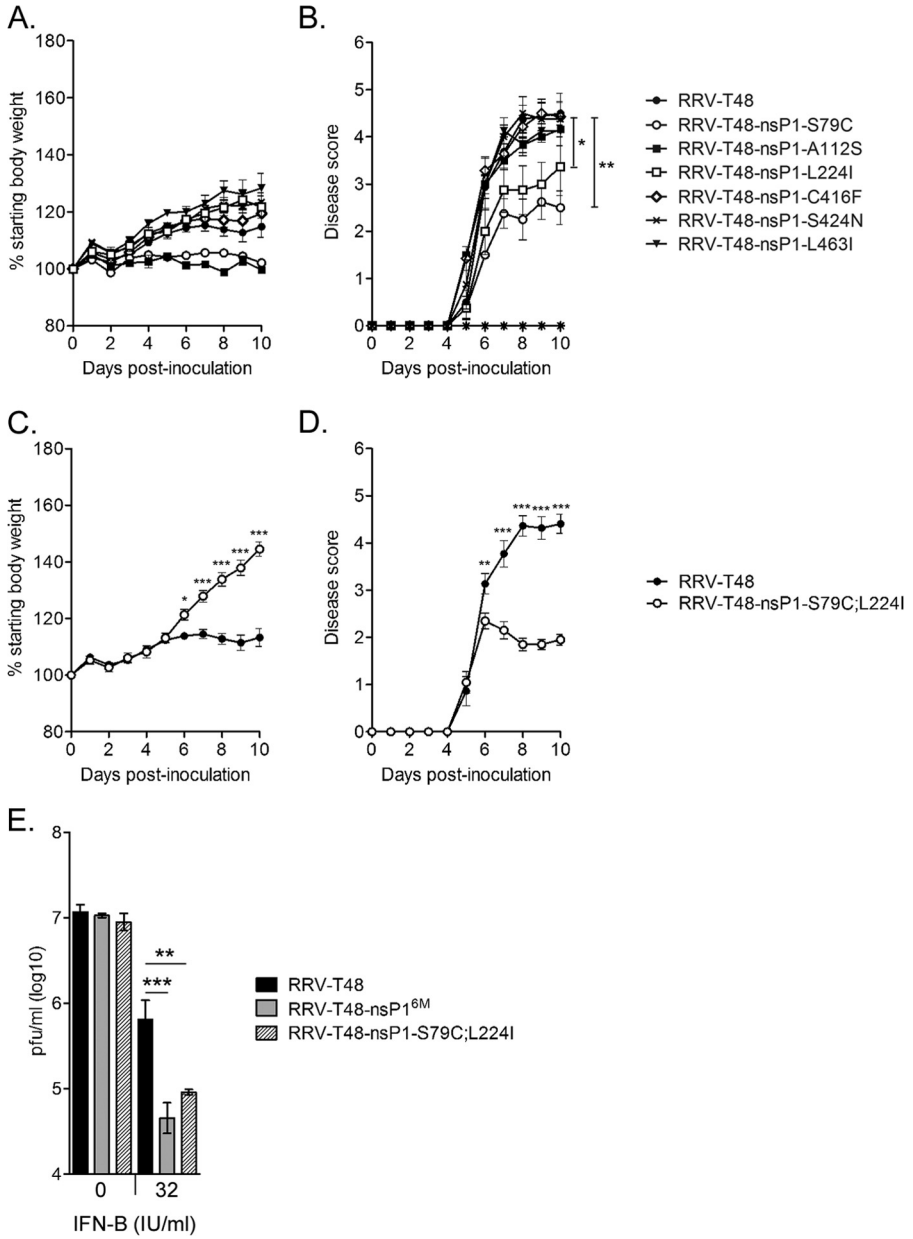

FIG 9 Mapping studies. (A and B) Three- to 4-week-old WT C57BL/6 mice were inoculated with 10^3 PFU of RRV T48 ($n = 8$), RRV-T48-nsP1-S79C ($n = 4$), RRV-T48-nsP1-A112S ($n = 3$), RRV-T48-nsP1-L224I ($n = 8$), RRV-T48-nsP1-C416F ($n = 7$), RRV-T48-nsP1-S424N ($n = 4$), or RRV-T48-nsP1-L463I ($n = 4$) by injection in the left rear footpad. At 24-h intervals, mice were assessed for weight gain (A) and were scored for musculoskeletal disease signs, including loss of gripping ability and altered gait (B). Each data point represents the arithmetic mean ± standard error of the mean. Data were evaluated for statistically significant differences by a repeated-measures ANOVA followed by Bonferroni's multiple-comparison test. *, $P < 0.05$; **, $P < 0.01$. (C and D) Three- to 4-week-old WT C57BL/6 mice were inoculated with 10^3 PFU of RRV T48 ($n = 11$) or RRV-T48-nsP1-S79C;L224I ($n = 10$) by injection in the left rear footpad. At 24-h intervals, mice were assessed for weight gain (C) and were scored for musculoskeletal disease signs, including loss of gripping ability and altered gait (D). Each data point represents the arithmetic mean ± standard error of the mean. Data were evaluated for statistically significant differences by a repeated-measures ANOVA, followed by Bonferroni's multiple-comparison test. *, $P < 0.05$; **, $P < 0.01$; ***, $P < 0.001$. (E) Virus yields at 48 hpi in Vero cells either left untreated or treated with 32 IU/ml of IFN-β 3 h after infection with RRV T48, RRV-T48-nsP1^{6M}, or RRV-T48-nsP1-S79C;L224I (MOI, 0.1). Asterisks indicate significant differences (**, $P < 0.01$; ***, $P < 0.001$) as determined by ANOVA followed by Tukey's multiple-comparison test.

the methyltransferase, and specific mutations that affect the binding of enzymatic substrates have been located in the first 310 amino acids of nsP1. For example, two conserved acidic residues, D62 and D88 in RRV nsP1, are essential for *S*-adenosyl-L-methionine binding (46). In addition, mutations in the N terminus of nsP1 (R87L and S88C) of SINV increased the affinity of nsP1 for *S*-adenosyl-L-methionine (48), and mutations at nsP1 residues 23 and 302 were selected during SINV replication in the presence of decreased levels of GTP, likely increasing the affinity of nsP1 for GTP (49). These studies indicate that specific mutations can modulate nsP1 methyltransferase and guanylyltransferase activities. As discussed further below, we hypothesize that the attenuating mu-

tations in nsP1 identified in this study modulate nsP1 function in RNA synthesis and/or capping activity in a manner that increases the effectiveness of IFN-stimulated antiviral effectors. Intriguingly, however, these effects appear to be operative in skeletal muscle tissue but not in joint-associated tissues. Alternatively, it is possible that the attenuating mutations in nsP1 affect some aspect of nonstructural polyprotein processing and the release of free nsP2, which plays important roles in counteracting the IFN response to alphavirus infection (50–52). However, previously published studies suggested that the kinetics of nonstructural polyprotein processing by RRV T48 and RRV-T48-nsP1^{DC5692}, though not tested in cells, were similar in an *in vitro* translation assay (25). Thus, further studies are needed to determine the precise mechanisms by which these mutations in nsP1 contribute to RRV virulence.

Attenuating mutations in nsP1 reveal that host control of RRV infection is tissue specific. Based on our experiments in WT mice, which indicated that the amounts of infectious virus in the tissues of mice inoculated with RRV T48 and RRV-T48-nsP1^{6M} were similar until 7 dpi, we hypothesized that RRV-T48-nsP1^{6M} was more susceptible to some aspect of the adaptive immune response. However, measurements of weight gain and musculoskeletal disease signs indicated that RRV-T48-nsP1^{6M} was attenuated in *Rag1*$^{-/-}$ mice. In addition, *Rag1*$^{-/-}$ mice infected with RRV-T48-nsP1^{6M} showed a tissue-specific pattern of infection, with RRV T48-nsP1^{6M} replicating to higher, equivalent, or lower titers than RRV T48 in the sera, ankles, or quadriceps muscle tissues, respectively. In both WT and *Rag1*$^{-/-}$ mice, we detected similar levels of RRV RNA in quadriceps muscle tissues at 3 dpi, a finding consistent with our analysis of viral loads by plaque assays. However, at both 5 and 7 dpi, RRV RNA levels in quadriceps muscles were dramatically lower in RRV-T48-nsP1^{6M}-infected WT and *Rag1*$^{-/-}$ mice than in RRV T48-infected mice. In contrast, RRV RNA levels in the ankles of WT mice at 7 dpi were equivalent (Fig. 5C and D). These data indicate that the attenuating mutations in nsP1 enhanced innate host control of RRV in skeletal muscle tissue but had no effect on RRV RNA levels in joint tissue.

Attenuating mutations in nsP1 enhance the sensitivity of RRV to type I IFN. Due to the timing of the differences between the loads of RRV T48 and RRV-T48-nsP1^{6M} in the skeletal muscle tissues of WT and *Rag1*$^{-/-}$ mice (after 3 dpi), and the correlation of these differences with the infiltration of skeletal muscle tissue with NK cells (15), we tested whether depletion of NK cells from WT and *Rag1*$^{-/-}$ mice or infection of mice deficient in IFN-γ, an antiviral effector molecule produced by NK cells and other cell types, would restore the loads of the nsP1 mutant virus in skeletal muscle tissue. However, neither of these strategies recovered loads of the nsP1 mutant virus in skeletal muscle tissue, suggesting that some other aspect of the innate response mediates the effects observed. Type I IFN is a critical regulator of alphavirus replication, spread, and virulence (36). Numerous studies have demonstrated that the outcome of infection with alphaviruses is more severe in mice with defects in the type I IFN response than in WT mice (53–62). We found that RRV T48 and RRV-T48-nsP1^{6M} were equally virulent in 3- to 4-week-old *Ifnar1*$^{-/-}$ C57BL/6 mice, suggesting that type I IFN responses contribute to the attenuation of the mutant virus RRV-T48-nsP1^{6M} in WT mice. Furthermore, when we inoculated older *Ifnar1*$^{-/-}$ mice with a low dose of virus (5 PFU) to extend survival time, we found that the RRV-T48 and RRV-T48-nsP1^{6M} loads in skeletal muscle tissues at 4 dpi were not significantly different (4- to 6-fold [P, >0.05]). Our measurements of type I IFN in the sera of WT mice indicated that RRV-T48-nsP1^{6M} was not a more potent inducer of type I IFN than RRV T48. However, *in vitro* type I IFN sensitivity assays demonstrated that both RRV-T48-nsP1^{6M} and RRV-T48-nsP1 S79C; L224I were more sensitive than RRV T48 to type I IFN. Recently, Lidbury et al. described a mutant RRV (RRV$_{PERS}$) isolated from persistently infected murine macrophages (63). In agreement with our findings, in which sensitivity to type I IFN *in vitro* correlated with pathogenicity *in vivo*, RRV$_{PERS}$ displayed increased virulence in mice and increased resistance to type I IFN *in vitro*. Five of the 12 amino acid differences between RRV T48 and RRV$_{PERS}$ were located in nsP1 (63). In addition, the mutations in nsP1 that arose during SINV passage in the presence of decreased levels of GTP also conferred enhanced sensitivity to interferon (49, 64). Taken together, these studies and the work reported here indicate that sequence variation in nsP1 may influence the resistance of RRV to the antiviral effects of type I IFN, and they suggest that modulation of nsP1 RNA-capping activity influences IFN sensitivity. In addition, our analyses of viral loads in distinct tissues of WT and *Rag1*$^{-/-}$ mice suggest that the mutations in nsP1 enhanced the sensitivity of RRV to type I IFN in a tissue-specific manner. These findings raise the possibility that some aspect of the type I IFN response that contributes to the control of RRV infection is defective in joint-associated tissues. Further investigation is needed in order to understand the basis for the tissue- and cell type-specific actions of type I IFN and the tissue-specific mechanisms that mediate the control of RRV infection.

ACKNOWLEDGMENTS

This research was supported by Public Health Service grant K22 AI079163, awarded to T.E.M. from the National Institute of Allergy and Infectious Diseases. H.J.J. and K.A.S.B. were supported by Public Health Service grant T32 AI052066 from the National Institute of Allergy and Infectious Diseases.

REFERENCES

1. **Powers AM, Brault AC, Shirako Y, Strauss EG, Kang W, Strauss JH, Weaver SC.** 2001. Evolutionary relationships and systematics of the alphaviruses. J. Virol. **75:**10118–10131. http://dx.doi.org/10.1128/JVI.75.21.10118-10131.2001.
2. **Harley D, Sleigh A, Ritchie S.** 2001. Ross River virus transmission, infection, and disease: a cross-disciplinary review. Clin. Microbiol. Rev. **14:**909–932. http://dx.doi.org/10.1128/CMR.14.4.909-932.2001.
3. **Williams MC, Woodall JP, Gillett JD.** 1965. O'nyong-nyong fever: an epidemic virus disease in East Africa. VII. Virus isolations from man and serological studies up to July 1961. Trans. R. Soc. Trop. Med. Hyg. **59:**186–197.
4. **Weaver SC, Reisen WK.** 2010. Present and future arboviral threats. Antiviral Res. **85:**328–345. http://dx.doi.org/10.1016/j.antiviral.2009.10.008.
5. **Pialoux G, Gauzere BA, Jaureguiberry S, Strobel M.** 2007. Chikungunya, an epidemic arbovirosis. Lancet Infect. Dis. **7:**319–327. http://dx.doi.org/10.1016/S1473-3099(07)70107-X.
6. **Pinheiro FP, Freitas RB, Travassos da Rosa JF, Gabbay YB, Mello WA, LeDuc JW.** 1981. An outbreak of Mayaro virus disease in Belterra, Brazil. I. Clinical and virological findings. Am. J. Trop. Med. Hyg. **30:**674–681.
7. **Staples JE, Breiman RF, Powers AM.** 2009. Chikungunya fever: an epidemiological review of a re-emerging infectious disease. Clin. Infect. Dis. **49:**942–948. http://dx.doi.org/10.1086/605496.
8. **Borgherini G, Poubeau P, Jossaume A, Gouix A, Cotte L, Michault A, Arvin-Berod C, Paganin F.** 2008. Persistent arthralgia associated with chikungunya virus: a study of 88 adult patients on Reunion Island. Clin. Infect. Dis. **47:**469–475. http://dx.doi.org/10.1086/590003.
9. **Brighton SW, Prozesky OW, de la Harpe AL.** 1983. Chikungunya virus infection. A retrospective study of 107 cases. S. Afr. Med. J. **63:**313–315.

10. **Larrieu S, Pouderoux N, Pistone T, Filleul L, Receveur MC, Sissoko D, Ezzedine K, Malvy D.** 2010. Factors associated with persistence of arthralgia among Chikungunya virus-infected travellers: report of 42 French cases. J. Clin. Virol. **47:**85–88. http://dx.doi.org/10.1016/j.jcv.2009.11.014.
11. **Simon F, Parola P, Grandadam M, Fourcade S, Oliver M, Brouqui P, Hance P, Kraemer P, Ali Mohamed A, de Lamballerie X, Charrel R, Tolou H.** 2007. Chikungunya infection: an emerging rheumatism among travelers returned from Indian Ocean islands. Report of 47 cases. Medicine (Baltimore) **86:**123–137. http://dx.doi.org/10.1097/MD/0b013e31806010a5.
12. **Sissoko D, Malvy D, Ezzedine K, Renault P, Moscetti F, Ledrans M, Pierre V.** 2009. Post-epidemic Chikungunya disease on Reunion Island: course of rheumatic manifestations and associated factors over a 15-month period. PLoS Negl. Trop. Dis. **3:**e389. http://dx.doi.org/10.1371/journal.pntd.0000389.
13. **Morrison TE, Fraser RJ, Smith PN, Mahalingam S, Heise MT.** 2007. Complement contributes to inflammatory tissue destruction in a mouse model of Ross River virus-induced disease. J. Virol. **81:**5132–5143. http://dx.doi.org/10.1128/JVI.02799-06.
14. **Morrison TE, Simmons JD, Heise MT.** 2008. Complement receptor 3 promotes severe Ross River virus-induced disease. J. Virol. **82:**11263–11272. http://dx.doi.org/10.1128/JVI.01352-08.
15. **Morrison TE, Whitmore AC, Shabman RS, Lidbury BA, Mahalingam S, Heise MT.** 2006. Characterization of Ross River virus tropism and virus-induced inflammation in a mouse model of viral arthritis and myositis. J. Virol. **80:**737–749. http://dx.doi.org/10.1128/JVI.80.2.737-749.2006.
16. **Morrison TE, Oko L, Montgomery SA, Whitmore AC, Lotstein AR, Gunn BM, Elmore SA, Heise MT.** 2011. A mouse model of chikungunya virus-induced musculoskeletal inflammatory disease: evidence of arthritis, tenosynovitis, myositis, and persistence. Am. J. Pathol. **178:**32–40. http://dx.doi.org/10.1016/j.ajpath.2010.11.018.
17. **Hawman DW, Stoermer KA, Montgomery SA, Pal P, Oko L, Diamond MS, Morrison TE.** 2013. Chronic joint disease caused by persistent Chikungunya virus infection is controlled by the adaptive immune response. J. Virol. **87:**13878–13888. http://dx.doi.org/10.1128/JVI.02666-13.
18. **Lidbury BA, Rulli NE, Suhrbier A, Smith PN, McColl SR, Cunningham AL, Tarkowski A, van Rooijen N, Fraser RJ, Mahalingam S.** 2008. Macrophage-derived proinflammatory factors contribute to the development of arthritis and myositis after infection with an arthrogenic alphavirus. J. Infect. Dis. **197:**1585–1593. http://dx.doi.org/10.1086/587841.
19. **Hoarau JJ, Jaffar Bandjee MC, Trotot PK, Das T, Li-Pat-Yuen G, Dassa B, Denizot M, Guichard E, Ribera A, Henni T, Tallet F, Moiton MP, Gauzere BA, Bruniquet S, Jaffar Bandjee Z, Morbidelli P, Martigny G, Jolivet M, Gay F, Grandadam M, Tolou H, Vieillard V, Debre P, Autran B, Gasque P.** 2010. Persistent chronic inflammation and infection by Chikungunya arthritogenic alphavirus in spite of a robust host immune response. J. Immunol. **184:**5914–5927. http://dx.doi.org/10.4049/jimmunol.0900255.
20. **Parola P, de Lamballerie X, Jourdan J, Rovery C, Vaillant V, Minodier P, Brouqui P, Flahault A, Raoult D, Charrel RN.** 2006. Novel chikungunya virus variant in travelers returning from Indian Ocean islands. Emerg. Infect. Dis. **12:**1493–1499. http://dx.doi.org/10.3201/eid1210.060610.
21. **Soden M, Vasudevan H, Roberts B, Coelen R, Hamlin G, Vasudevan S, La Brooy J.** 2000. Detection of viral ribonucleic acid and histologic analysis of inflamed synovium in Ross River virus infection. Arthritis Rheum. **43:**365–369. http://dx.doi.org/10.1002/1529-0131(200002)43:2<365::AID-ANR16>3.0.CO;2-E.
22. **Fraser JR, Cunningham AL, Clarris BJ, Aaskov JG, Leach R.** 1981. Cytology of synovial effusions in epidemic polyarthritis. Aust. N. Z. J. Med. **11:**168–173. http://dx.doi.org/10.1111/j.1445-5994.1981.tb04226.x.
23. **Ozden S, Huerre M, Riviere JP, Coffey LL, Afonso PV, Mouly V, de Monredon J, Roger JC, El Amrani M, Yvin JL, Jaffar MC, Frenkiel MP, Sourisseau M, Schwartz O, Butler-Browne G, Despres P, Gessain A, Ceccaldi PE.** 2007. Human muscle satellite cells as targets of Chikungunya virus infection. PLoS One **2:**e527. http://dx.doi.org/10.1371/journal.pone.0000527.
24. **Hazelton RA, Hughes C, Aaskov JG.** 1985. The inflammatory response in the synovium of a patient with Ross River arbovirus infection. Aust. N. Z. J. Med. **15:**336–339. http://dx.doi.org/10.1111/j.1445-5994.1985.tb04048.x.
25. **Jupille HJ, Oko L, Stoermer KA, Heise MT, Mahalingam S, Gunn BM, Morrison TE.** 2011. Mutations in nsP1 and PE2 are critical determinants of Ross River virus-induced musculoskeletal inflammatory disease in a mouse model. Virology **410:**216–227. http://dx.doi.org/10.1016/j.virol.2010.11.012.
26. **Dalgarno L, Rice CM, Strauss JH.** 1983. Ross River virus 26 S RNA: complete nucleotide sequence and deduced sequence of the encoded structural proteins. Virology **129:**170–187. http://dx.doi.org/10.1016/0042-6822(83)90404-X.
27. **Kuhn RJ, Niesters HG, Hong Z, Strauss JH.** 1991. Infectious RNA transcripts from Ross River virus cDNA clones and the construction and characterization of defined chimeras with Sindbis virus. Virology **182:**430–441. http://dx.doi.org/10.1016/0042-6822(91)90584-X.
28. **Lindsay M, Oliveira N, Jasinska E, Johansen C, Harrington S, Wright AE, Smith D.** 1996. An outbreak of Ross River virus disease in Southwestern Australia. Emerg. Infect. Dis. **2:**117–120. http://dx.doi.org/10.3201/eid0202.960206.
29. **Stoermer KA, Burrack A, Oko L, Montgomery SA, Borst LB, Gill RG, Morrison TE.** 2012. Genetic ablation of arginase 1 in macrophages and neutrophils enhances clearance of an arthritogenic alphavirus. J. Immunol. **189:**4047–4059. http://dx.doi.org/10.4049/jimmunol.1201240.
30. **Beilke JN, Kuhl NR, Van Kaer L, Gill RG.** 2005. NK cells promote islet allograft tolerance via a perforin-dependent mechanism. Nat. Med. **11:**1059–1065. http://dx.doi.org/10.1038/nm1296.
31. **Swiecki M, Gilfillan S, Vermi W, Wang Y, Colonna M.** 2010. Plasmacytoid dendritic cell ablation impacts early interferon responses and antiviral NK and $CD8^+$ T cell accrual. Immunity **33:**955–966. http://dx.doi.org/10.1016/j.immuni.2010.11.020.
32. **Shabman RS, Morrison TE, Moore C, White L, Suthar MS, Hueston L, Rulli N, Lidbury B, Ting JP, Mahalingam S, Heise MT.** 2007. Differential induction of type I interferon responses in myeloid dendritic cells by mosquito and mammalian-cell-derived alphaviruses. J. Virol. **81:**237–247. http://dx.doi.org/10.1128/JVI.01590-06.
33. **Meager A.** 2002. Biological assays for interferons. J. Immunol. Methods **261:**21–36. http://dx.doi.org/10.1016/S0022-1759(01)00570-1.
34. **Mombaerts P, Iacomini J, Johnson RS, Herrup K, Tonegawa S, Papaioannou VE.** 1992. RAG-1-deficient mice have no mature B and T lymphocytes. Cell **68:**869–877. http://dx.doi.org/10.1016/0092-8674(92)90030-G.
35. **Biron CA, Brossay L.** 2001. NK cells and NKT cells in innate defense against viral infections. Curr. Opin. Immunol. **13:**458–464. http://dx.doi.org/10.1016/S0952-7915(00)00241-7.
36. **Ryman KD, Klimstra WB.** 2008. Host responses to alphavirus infection. Immunol. Rev. **225:**27–45. http://dx.doi.org/10.1111/j.1600-065X.2008.00670.x.
37. **Emeny JM, Morgan MJ.** 1979. Regulation of the interferon system: evidence that Vero cells have a genetic defect in interferon production. J. Gen. Virol. **43:**247–252. http://dx.doi.org/10.1099/0022-1317-43-1-247.
38. **Mosca JD, Pitha PM.** 1986. Transcriptional and posttranscriptional regulation of exogenous human beta interferon gene in simian cells defective in interferon synthesis. Mol. Cell. Biol. **6:**2279–2283.
39. **Strauss JH, Strauss EG.** 1994. The alphaviruses: gene expression, replication, and evolution. Microbiol. Rev. **58:**491–562.
40. **Wang HL, O'Rear J, Stollar V.** 1996. Mutagenesis of the Sindbis virus nsP1 protein: effects on methyltransferase activity and viral infectivity. Virology **217:**527–531. http://dx.doi.org/10.1006/viro.1996.0147.
41. **Tomar S, Narwal M, Harms E, Smith JL, Kuhn RJ.** 2011. Heterologous production, purification and characterization of enzymatically active Sindbis virus nonstructural protein nsP1. Protein Expr. Purif. **79:**277–284. http://dx.doi.org/10.1016/j.pep.2011.05.022.
42. **Faragher SG, Meek AD, Rice CM, Dalgarno L.** 1988. Genome sequences of a mouse-avirulent and a mouse-virulent strain of Ross River virus. Virology **163:**509–526. http://dx.doi.org/10.1016/0042-6822(88)90292-9.
43. **Lulla V, Sawicki DL, Sawicki SG, Lulla A, Merits A, Ahola T.** 2008. Molecular defects caused by temperature-sensitive mutations in Semliki Forest virus nsP1. J. Virol. **82:**9236–9244. http://dx.doi.org/10.1128/JVI.00711-08.
44. **Wang YF, Sawicki SG, Sawicki DL.** 1991. Sindbis virus nsP1 functions in negative-strand RNA synthesis. J. Virol. **65:**985–988.
45. **Ahola T, Kaariainen L.** 1995. Reaction in alphavirus mRNA capping: formation of a covalent complex of nonstructural protein nsP1 with 7-methyl-GMP. Proc. Natl. Acad. Sci. U. S. A. **92:**507–511. http://dx.doi.org/10.1073/pnas.92.2.507.
46. **Ahola T, Laakkonen P, Vihinen H, Kaariainen L.** 1997. Critical residues

of Semliki Forest virus RNA capping enzyme involved in methyltransferase and guanylyltransferase-like activities. J. Virol. **71:**392–397.
47. **Mi S, Durbin R, Huang HV, Rice CM, Stollar V.** 1989. Association of the Sindbis virus RNA methyltransferase activity with the nonstructural protein nsP1. Virology **170:**385–391. http://dx.doi.org/10.1016/0042-6822(89)90429-7.
48. **Scheidel LM, Durbin RK, Stollar V.** 1989. SVLM21, a Sindbis virus mutant resistant to methionine deprivation, encodes an altered methyltransferase. Virology **173:**408–414. http://dx.doi.org/10.1016/0042-6822(89)90553-9.
49. **Scheidel LM, Stollar V.** 1991. Mutations that confer resistance to mycophenolic acid and ribavirin on Sindbis virus map to the nonstructural protein nsP1. Virology **181:**490–499. http://dx.doi.org/10.1016/0042-6822(91)90881-B.
50. **Gorchakov R, Frolova E, Sawicki S, Atasheva S, Sawicki D, Frolov I.** 2008. A new role for ns polyprotein cleavage in Sindbis virus replication. J. Virol. **82:**6218–6231. http://dx.doi.org/10.1128/JVI.02624-07.
51. **Frolova EI, Fayzulin RZ, Cook SH, Griffin DE, Rice CM, Frolov I.** 2002. Roles of nonstructural protein nsP2 and alpha/beta interferons in determining the outcome of Sindbis virus infection. J. Virol. **76:**11254–11264. http://dx.doi.org/10.1128/JVI.76.22.11254-11264.2002.
52. **Fros JJ, Liu WJ, Prow NA, Geertsema C, Ligtenberg M, Vanlandingham DL, Schnettler E, Vlak JM, Suhrbier A, Khromykh AA, Pijlman GP.** 2010. Chikungunya virus nonstructural protein 2 inhibits type I/II interferon-stimulated JAK-STAT signaling. J. Virol. **84:**10877–10887. http://dx.doi.org/10.1128/JVI.00949-10.
53. **Gardner CL, Burke CW, Higgs ST, Klimstra WB, Ryman KD.** 2012. Interferon-alpha/beta deficiency greatly exacerbates arthritogenic disease in mice infected with wild-type chikungunya virus but not with the cell culture-adapted live-attenuated 181/25 vaccine candidate. Virology **425:**103–112. http://dx.doi.org/10.1016/j.virol.2011.12.020.
54. **Gardner CL, Yin J, Burke CW, Klimstra WB, Ryman KD.** 2009. Type I interferon induction is correlated with attenuation of a South American eastern equine encephalitis virus strain in mice. Virology **390:**338–347. http://dx.doi.org/10.1016/j.virol.2009.05.030.
55. **Ryman KD, Klimstra WB, Nguyen KB, Biron CA, Johnston RE.** 2000. Alpha/beta interferon protects adult mice from fatal Sindbis virus infection and is an important determinant of cell and tissue tropism. J. Virol. **74:**3366–3378. http://dx.doi.org/10.1128/JVI.74.7.3366-3378.2000.
56. **Ryman KD, Meier KC, Gardner CL, Adegboyega PA, Klimstra WB.** 2007. Non-pathogenic Sindbis virus causes hemorrhagic fever in the absence of alpha/beta and gamma interferons. Virology **368:**273–285. http://dx.doi.org/10.1016/j.virol.2007.06.039.
57. **Wollish AC, Ferris MT, Blevins LK, Loo YM, Gale M, Jr, Heise MT.** 2013. An attenuating mutation in a neurovirulent Sindbis virus strain interacts with the IPS-1 signaling pathway in vivo. Virology **435:**269–280. http://dx.doi.org/10.1016/j.virol.2012.09.008.
58. **White LJ, Wang JG, Davis NL, Johnston RE.** 2001. Role of alpha/beta interferon in Venezuelan equine encephalitis virus pathogenesis: effect of an attenuating mutation in the 5′ untranslated region. J. Virol. **75:**3706–3718. http://dx.doi.org/10.1128/JVI.75.8.3706-3718.2001.
59. **Rudd PA, Wilson J, Gardner J, Larcher T, Babarit C, Le TT, Anraku I, Kumagai Y, Loo YM, Gale M, Jr, Akira S, Khromykh AA, Suhrbier A.** 2012. Interferon response factors 3 and 7 protect against Chikungunya virus hemorrhagic fever and shock. J. Virol. **86:**9888–9898. http://dx.doi.org/10.1128/JVI.00956-12.
60. **Schilte C, Buckwalter MR, Laird ME, Diamond MS, Schwartz O, Albert ML.** 2012. Independent roles for IRF-3 and IRF-7 in hematopoietic and nonhematopoietic cells during host response to Chikungunya infection. J. Immunol. **188:**2967–2971. http://dx.doi.org/10.4049/jimmunol.1103185.
61. **Schilte C, Couderc T, Chretien F, Sourisseau M, Gangneux N, Guivel-Benhassine F, Kraxner A, Tschopp J, Higgs S, Michault A, Arenzana-Seisdedos F, Colonna M, Peduto L, Schwartz O, Lecuit M, Albert ML.** 2010. Type I IFN controls chikungunya virus via its action on nonhematopoietic cells. J. Exp. Med. **207:**429–442. http://dx.doi.org/10.1084/jem.20090851.
62. **Couderc T, Chretien F, Schilte C, Disson O, Brigitte M, Guivel-Benhassine F, Touret Y, Barau G, Cayet N, Schuffenecker I, Despres P, Arenzana-Seisdedos F, Michault A, Albert ML, Lecuit M.** 2008. A mouse model for Chikungunya: young age and inefficient type-I interferon signaling are risk factors for severe disease. PLoS Pathog. **4:**e29. http://dx.doi.org/10.1371/journal.ppat.0040029.
63. **Lidbury BA, Rulli NE, Musso CM, Cossetto SB, Zaid A, Suhrbier A, Rothenfluh HS, Rolph MS, Mahalingam S.** 2011. Identification and characterization of a Ross River virus variant that grows persistently in macrophages, shows altered disease kinetics in a mouse model, and exhibits resistance to type I interferon. J. Virol. **85:**5651–5663. http://dx.doi.org/10.1128/JVI.01189-10.
64. **Rosenblum CI, Stollar V.** 1999. SVMPA, a mutant of Sindbis virus resistant to mycophenolic acid and ribavirin, shows an increased sensitivity to chick interferon. Virology **259:**228–233. http://dx.doi.org/10.1006/viro.1999.9775.